Reply

W. WISCOMBE

NASA/Goddard Space Flight Center, Laboratory for Atmospheres, Greenbelt, MD 20771

R. WELCH

Institute of Atmospheric Sciences, South Dakota School of Mines and Technology, Rapid City, SD 57701

3 September 1985

1. Introduction

Professor Hegg has pointed out that Wiscombe et al. (1984; hereinafter WWH) were too conservative in their choice of effective droplet radius (r_{eff}). Hegg notes that he and other investigators have frequently measured effective radii of several hundred microns in nonprecipitating clouds, while our largest value was only 55 μm.

But while we were too conservative for a cloud physicist, we are too liberal for many of our colleagues in cloud radiation, who prefer to ignore large drops in their calculations. When pressed to explain this omission, they will usually object that large drops must fall out of clouds rapidly. In some cases, they also face a practical constraint—spectrally detailed, single-scattering computations with large drops are beyond their computer budgets. We will deal with each of these issues below.

Figure 1 provides an illustration of the problem we are discussing. In the left-hand part is the "classic" Deirmendjian C.1 cloud-drop distribution (Deirmendjian, 1969). Drop distributions like this, lacking any drops bigger than 20–30 μm, are used by virtually all shortwave/longwave cloud-radiation modelers. In the right-hand part of Fig. 1 are three Marshall–Palmer raindrop distributions (Houze et. al., 1979); two are "classic" Marshall-Palmers with rain rates of 1 and 10 mm h^{-1}, while the third is the tail of the "large-drop" distribution from WWH. These are the types of drop distributions used by virtually all microwave cloud-radiation modelers. As Fig. 1 shows, droplets with radii between roughly 30 and 500 μm are in a sort of limbo. Yet they are undoubtedly present in a great many clouds, as both the observations of Hegg and the observations cited in WWH indicate.

In WWH, we provided evidence that neglecting drops with radii greater than 30 μm is ill-advised for shortwave modelers. We will now supplement that evidence, based on Hegg's comments, and show that large drops are, if anything, even more important for longwave modelers.

2. Adding a third ("very-large") drop distribution

Originally, we included 12 drop distributions in our study. The final one, which we call "very-large", evolved in the rising-parcel cloud model only 160 sec after the "large" drop distribution, and had an effective radius (r_{eff}) of 216 μm—about four times the r_{eff} of the large drop distribution—but a mean radius of only 16 μm. It represented almost the last model time step before significant amounts of liquid water began to be lost by evolution of drops out of the largest radius category. (Recall that the model had no breakup scheme whereby these drops could be recycled into smaller drops.) The very-large liquid water distribution is shown in Fig. 2, along with the original two distributions (normal and large) from WWH. Note that the major difference between the large and very-large distributions occurs for radii above 300 μm. The very-large distribution is still only monomodal on a plot of *concentration* vs radius, however.

In order to avoid charges of extremism, we eliminated all curves referring to this very-large drop distribution. Now, however, Hegg has cited measurements of r_{eff} up to 275 μm in nonprecipitating clouds. Furthermore, he maintains that such high values are not at all unusual. Thus, we wish to restore the very-large drop case in a few of the WWH curves.

3. Total shortwave absorptivity

Figure 3 is identical to Fig. 6 of WWH except that dashed curves for the very-large drop case have been added. The very-large drop results confirm, qualitatively, what was already evident in the large drop case. For overhead (top row in Fig. 3) and nearly overhead sun, the order of the curves changes as liquid water path (LWP) increases: for LWPs below about 500 g m^{-2} or so, larger drops mean *lower* absorptivity, while above 500 g m^{-2} the reverse is true. Only for larger solar zenith angles does this crossover effect disappear; then, for a given LWP, larger drops *always* mean higher absorptivity.

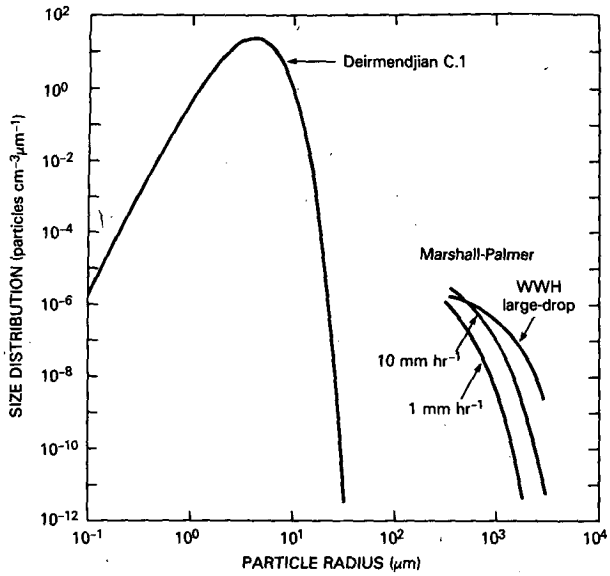

FIG. 1. Typical size distributions used in cloud radiation modeling.

The most important new result in the very-large case is that significantly larger absorptivities can now be obtained. (This was alluded to in the concluding section of WWH.) Enhancements of up to 0.08 over the normal case are possible, depending on LWP and sun angle. *This forces us to modify our conclusion in WWH that absorptivity enhancements due to large drops are not dramatic;* indeed, for larger LWPs and/or larger solar zenith angles, these enhancements would definitely be of climatological significance, and might explain some of the anomalously high values reported in aircraft experiments.

A final point about Fig. 3 is that the absorptivity in the very-large drop case shows no signs of reaching an asymptote as LWP increases. Beyond LWP = 100 g m^{-2} or so, very-large absorptivity grows roughly linearly in ln(LWP), long after the smaller-drop cases have more or less reached asymptotes. If LWP increases beyond the largest value considered (4000 g m^{-2}), the spread between the normal and very-large drop absorptivities will rise dramatically beyond the value of 0.08 quoted above.

4. Spectral albedo

Figure 4 is identical to Fig. 7 of WWH except that a new curve for very-large drops has been added, falling at every wavelength below the normal and large drop curves but above the clear-sky curve. Since each curve refers to the same liquid water path (see WWH for this and other qualifications), concentrations of only a few per cubic centimeter were necessary in the very-large case. Hence the very-large drop albedos are relatively low and have both a strong solar zenith angle dependence and a relatively strong spectral dependence in the 0.3–0.6 μm region, compared to the other two cloud cases. However, compared to the average cloudy atmospheric albedo of 50%, the very-large drop albedos do not seem anomalously low; and the slight coloration in the visible region would not be apparent to the naked eye.

5. Infrared cooling rate near cloud top

All the calculations in WWH were carried out for the longwave as well as the shortwave, but the longwave results were omitted for brevity. However, adding the very-large drop case now makes these results especially interesting.

Table 1 shows longwave cooling rate averaged over the top 50 m, the top 100 m, etc. of a cloud. The 2- and 4-km-thick cloud cases were specified in WWH; the 8-km-thick case was constructed in exact analogy with the thinner clouds. All three clouds used the "nominal" liquid water profiles plotted in Fig. 3 of WWH (for the 2- and 4-km thick clouds). The geometric thickness of the cloud is not particularly important in the longwave, however, because the cloud is so highly absorbing; the results in Table 1 would be unchanged if the liquid water content was set to zero starting 1 km below cloud top.

The main conclusion to be drawn from Table 1 is that averaging deeper and deeper into a cloud rapidly diminishes the effect of drop distribution. If 50- or 100-m resolution is necessary, then the effect of drop distribution is gigantic; uncertainty in the drop distribution can cause a factor of 5 variation in the cooling rate, even though the liquid water profile doesn't change. Yet if 500-m resolution is sufficient, drop distribution is of negligible importance in going from

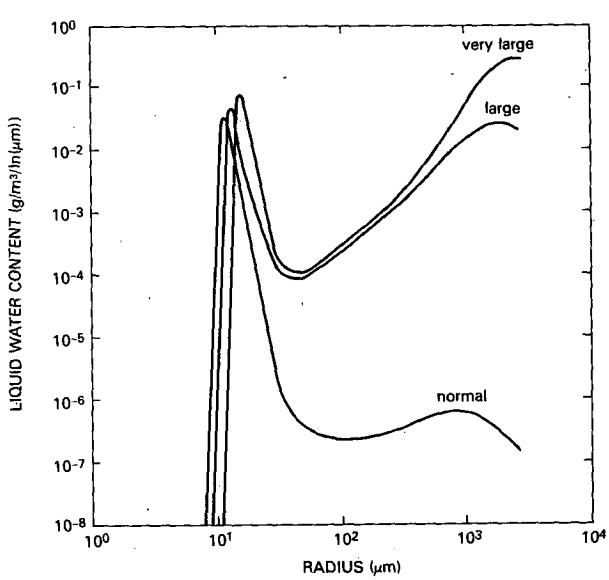

FIG. 2. Liquid water content distributions for the three drop distributions selected from the evolving-parcel cloud model of WWH

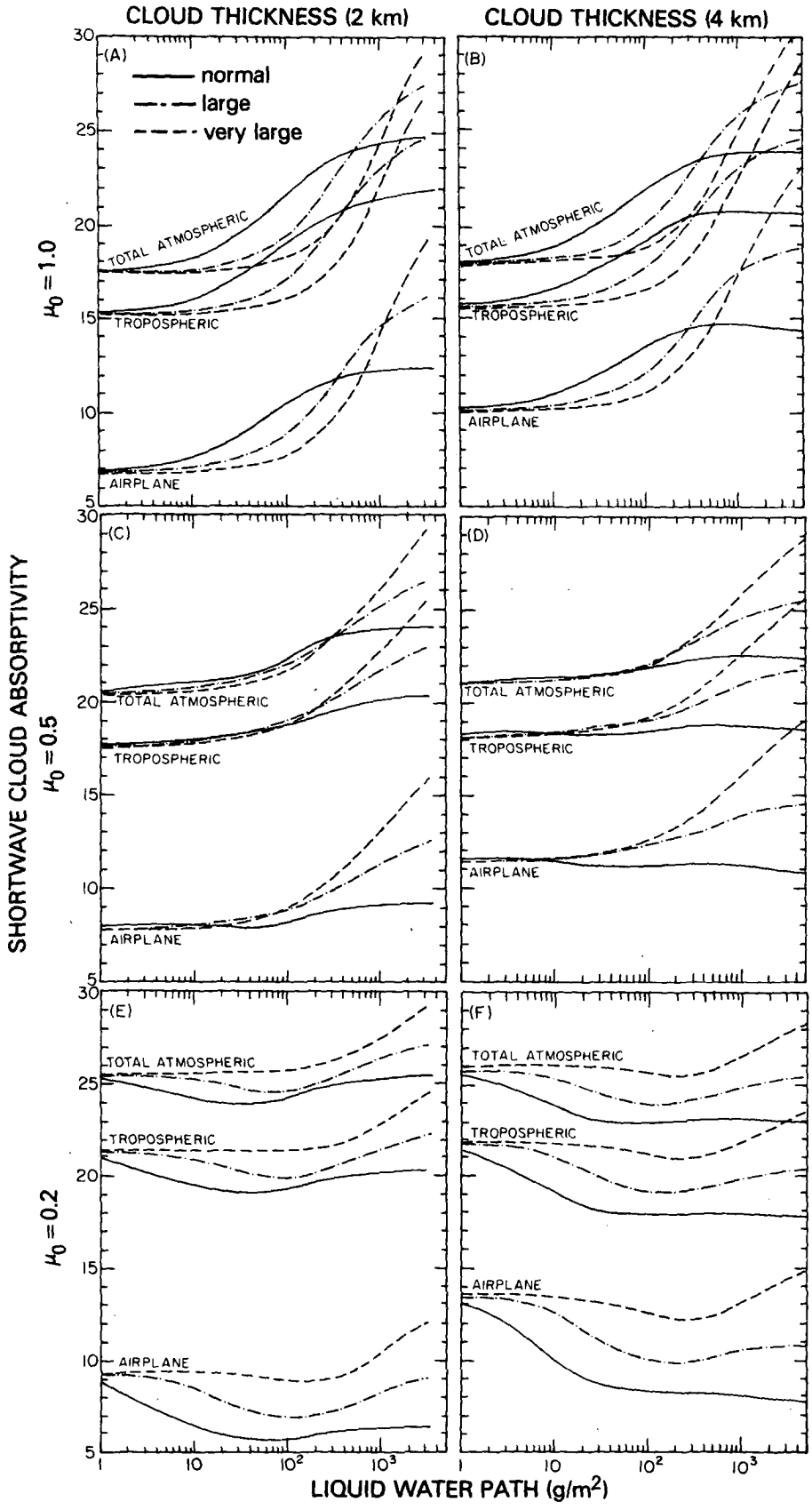

FIG. 3. Airplane (cloud-top-to-surface), tropospheric and total column absorptivities vs liquid water path for cloud thicknesses of 2 and 4 km and three solar zenith angles.

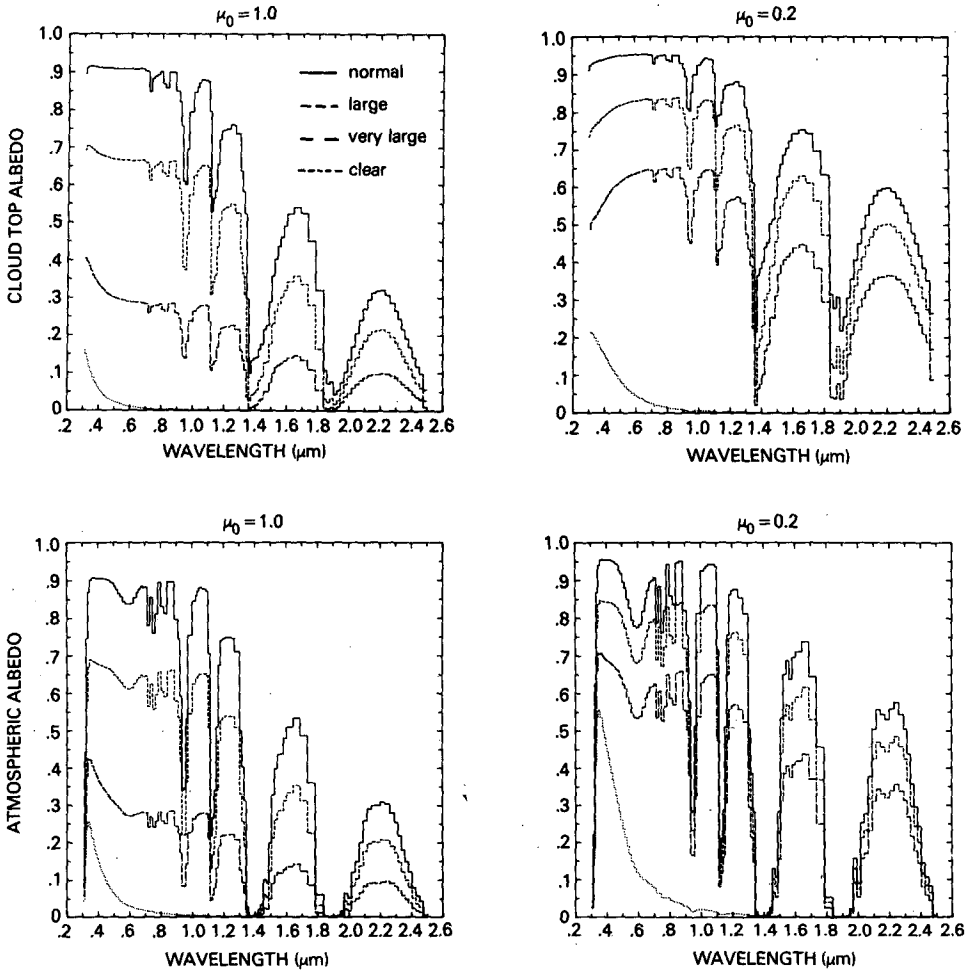

FIG. 4. Spectral albedo in 2-km-thick cloud case for two solar zenith angles. Top row is for cloud top, bottom row is for top of atmosphere (50 km). Drop distribution is uniform throughout the cloud.

normal to large, and of no more than 40% influence in going from normal or large to very-large.

6. Vertical variation of drop distribution

It is unlikely that an *entire* cloud would be made up of very large drops for long periods of time, for then there would be too few small drops to break up the large drops, and the large drops would just fall out. In practice, large drops will tend to be confined to the upper reaches of clouds, as Hegg's observations indicate. In an attempt to account for these observations, we have done a few new calculations in which the lower 1 km of a 2-km-thick cloud always has the normal drop distribution while the upper 1 km has either the normal, large or very-large distribution. The liquid water profile remains fixed at the values shown in Fig. 3 of WWH for all three of these cases. This is still a highly schematic representation of vertical drop distribution variability, but it is at least a step toward greater realism, without unduly complexifying the problem.

Cloud top and total atmospheric absorptivity and albedo for such a half-and-half cloud are given in Table 2. Cloud top albedo is reduced by about 0.1 at all sun angles, and even total albedo is reduced by 0.1 for overhead sun, when very-large drops replace normal drops in the top half of the cloud. This result was somewhat surprising, as one might expect the lower km of normal drops to determine the albedo, with the upper km having little impact no matter what its drop distribution.

In order to explain this result, we must turn to Fig. 5, which shows the spectral albedo for the three half-and-half cases. Figure 5 is arranged exactly like Fig. 4, although the behavior of the curves is quite different—Fig. 5 shows much less variability than Fig. 4 in the visible region, but only slightly less variability in the near-infrared region. Thus the development of large drops in the upper reaches of a cloud should give a

TABLE 1. Longwave (5–500 μm) cooling rates computed for model clouds of thickness 2, 4 and 8 km, and having either "normal" (N), "large" (L), or "very-large" (VL) drop distributions.

	IR cooling rates (K day^{-1})								
	2 km thick			4 km thick			8 km thick		
Cloud region	N	L	VL	N	L	VL	N	L	VL
top 50 m	85	30	15	71	27	17	82	33	22
top 100 m	92	42	19	89	36	18	112	43	23
top 250 m	46	41	24	63	44	23	96	56	27
top 500 m	23	23	19	32	31	23	50	47	29

very clear signal: the near-infrared albedo should plummet dramatically compared to the visible albedo. As far as the fall in total shortwave albedo is concerned, however, the two spectral regions have about equal effects, since most of the solar flux is concentrated in the visible region.

The changes in absorptivity revealed in Table 2, while not as large as in the case where the entire cloud has a large-drop distribution, are still substantial—0.03–0.05 in cloud-top-to-surface absorptivity and about 0.03 in total column absorptivity. For overhead sun, the biggest jump in absorptivity occurs in going from normal to large drops; there is little further increase in going on to very-large drops. But for sun angles of 60° and 78.5°, going from large to very-large drops causes further substantial increases in absorptivity. Thus the effect of large drops on absorptivity (and also albedo) can be expected to vary with latitude and season.

Figure 6 shows the combined shortwave plus longwave heating rate profiles for the three half-and-half clouds. The histogram form indicates the model vertical resolution. For $\mu_0 = 0.2$, corresponding to a sun angle of 78.5°, there is mostly cloud top longwave cooling which is extremely sensitive to the drop distribution, as we found also in Table 1. For overhead sun, however, we see in addition to the cloud top longwave cooling a peak of shortwave heating inside the cloud. The magnitude and geometric width of this heating–cooling couplet is very sensitive to the drop distribution.

7. The objection that large drops fall out

Some investigators have difficulty with the idea of large drops existing in clouds for extended time periods, because they know that millimeter-sized drops fall at several meters per sec. Without strong updrafts, which are unlikely except in vigorous cumuli, such drops must fall out—so the argument goes.

This seemingly plausible objection ignores two things, however. First, many observations, cited in WWH, show large drops existing for long periods in nonprecipitating clouds. Second, it assumes large drops are free to fall out of clouds without any impediment whatsoever. This entirely ignores drop breakup (Pruppacher and Klett, 1980), whereby, due mostly to collisions with smaller (and therefore slower moving) drops, but sometimes to aerodynamic instability as well, large drops are fragmented. This important mechanism is just beginning to receive the attention it deserves, and is certainly a frontier research problem in cloud physics. If, as the observations seem to imply, the time scale for breakup is rapid compared with the time it would take a large drop to fall out of a cloud, then it is easy to sustain a semipermanent large-drop population even with only weak updrafts.

In our opinion, based on the observational evidence we have seen, most clouds develop a population of large drops (with radii between 30 and 1000 μm). The largest of these drops would qualify as drizzle, although not as rain. But in most cases breakup is so powerful a mechanism that the cloud does not proceed to the rain stage. Rain represents an occasional failure of the breakup process, due to an insufficient number of small drops—or an overwhelming of the breakup process, due to a negatively buoyant downdraft or some such instability.

8. Single-scattering computation time

No one is more aware of the high cost of single-scattering (Mie) computations than ourselves. We have had to use uncounted hours of computer time on such computations, even with the advent of supercomputers like the CRAY. Even ignoring large drops and using a Deirmendjian C.1 drop distribution (Fig. 1) with a 30 μm cutoff can require a 1/2 h CRAY computation to produce a Mie scattering table for ATRAD (the radiation model used in WWH). Since computer time for exact Mie scattering calculations increases linearly with

TABLE 2. Shortwave (0.2–4.0 μm) absorptivity and albedo for a 2-km thick cloud with a fixed liquid water profile, a total liquid water path of 866 gm^{-2}, and a lower half always with a "normal" drop distribution. The liquid water profile peaks at 2.5 km rather than at 2.75 km as in WWH. θ is solar zenith angle.

Drop distribution, top 1/2 of cloud	θ = 78.5°	θ = 60°	θ = 0	θ = 78.5°	θ = 60°	θ = 0
	Cloud-top-to-surface absorptivity			*Cloud-top albedo*		
normal	6.4%	9.3%	12.4%	89.7%	85.5%	80.2%
large	8.6	11.9	15.2	84.7	79.1	72.1
very-large	11.0	13.9	15.9	81.2	75.6	69.2
	Total column absorptivity			*Top-of-atmosphere albedo*		
normal	24.9	23.6	24.4	72.2	71.9	69.0
large	26.4	25.6	26.4	68.5	66.7	62.1
very-large	28.1	27.1	26.9	66.0	63.9	59.7

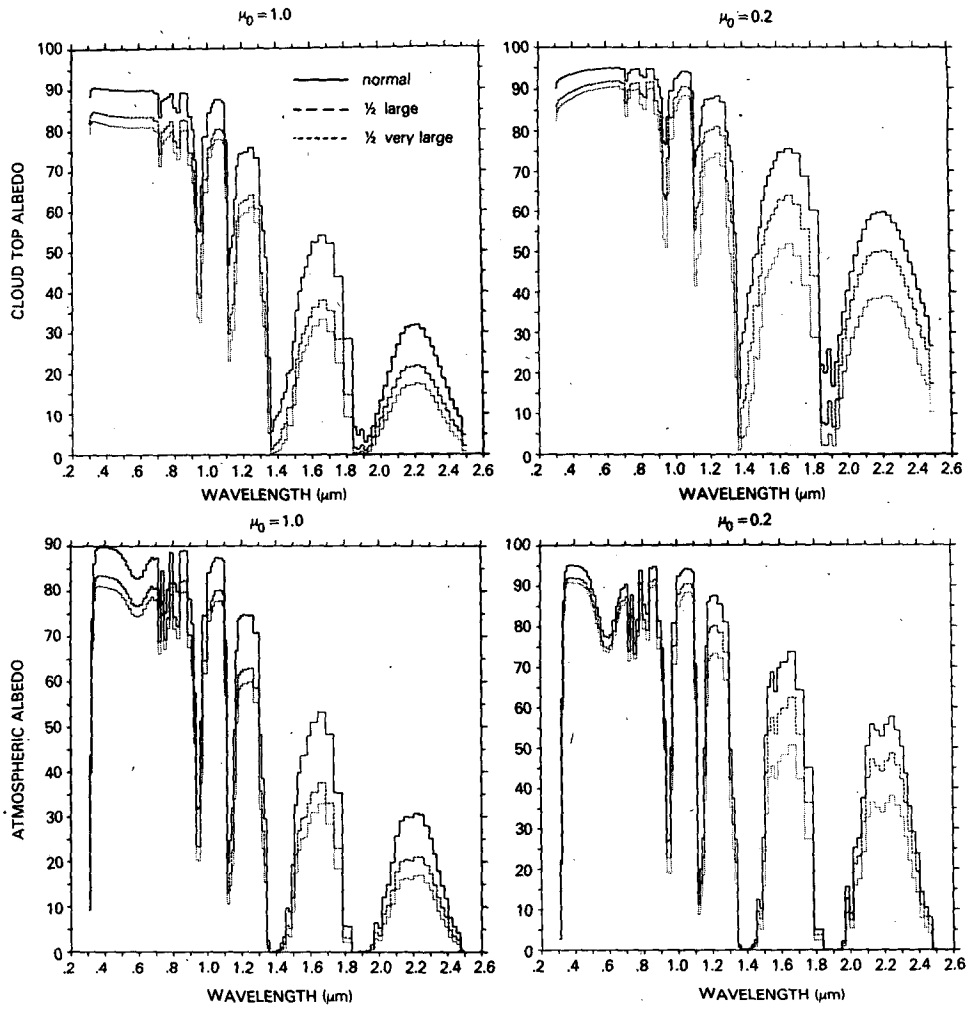

FIG. 5. Spectral albedo in 2-km-thick cloud case for two solar zenith angles. Top row is for cloud top, bottom row is for top of atmosphere (50 km). Drop distribution is always normal in lower half of cloud, and either normal, large or very-large in upper half.

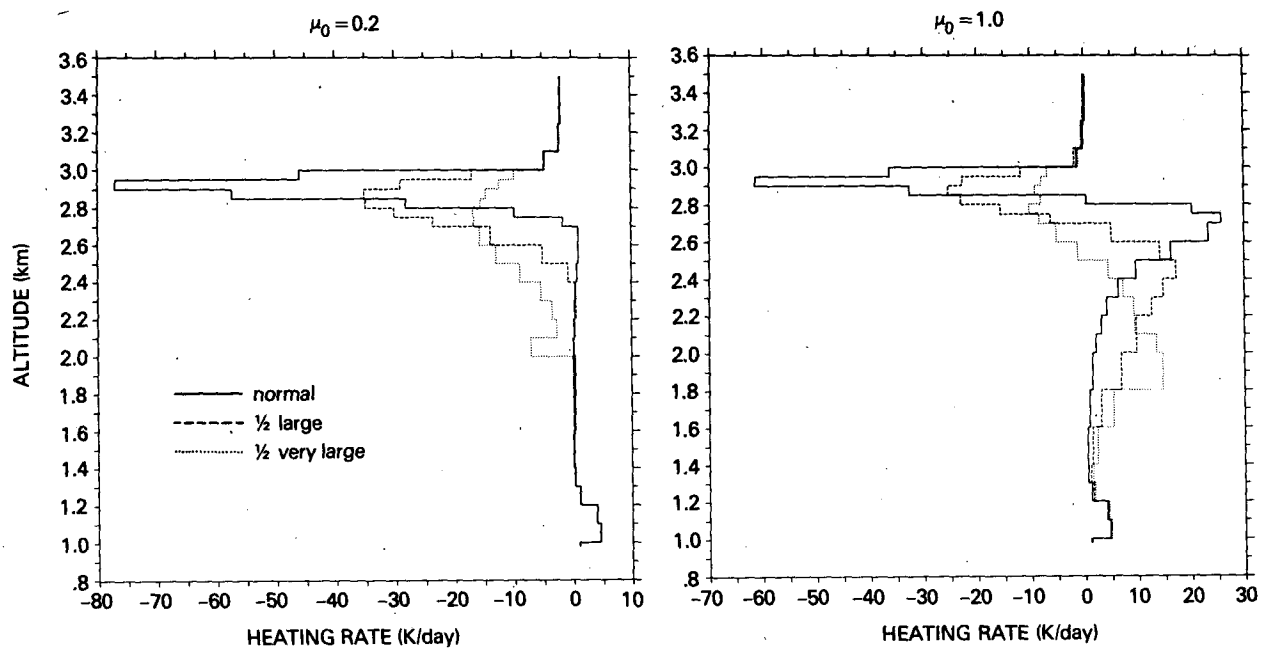

FIG. 6. Vertical profiles of total radiative heating rate (shortwave plus longwave) for two solar zenith angles and the 2-km-thick cloud. Drop distribution is always normal in lower half of cloud, and either normal, large or very-large in upper half.

drop size, it is clear that carrying such calculations up to 1000 μm instead of 30 μm is beyond the reach of most investigators.

This was the exact reason for resorting to the Complex Angular Momentum approximations to exact Mie theory (Nussenzweig and Wiscombe, 1980) in WWH. Unfortunately, we have not yet completed these approximations for the exact phase function, but at least we were able to get the asymmetry factor and hence use the Henyey-Greenstein phase function. Thus there is a viable way to avoid exorbitant costs for Mie calculations, if and when cloud radiation modelers wish to avail themselves of it.

A second approach that should be taken is to adopt standard formats for the interchange of single-scattering data. Then, investigators with access to supercomputers can create tables of such data that any other investigator, even of modest means, can use to make ATRAD-like calculations. Since the variables describing the single-scattering process are well known, it seems long past time to adopt such formats.

9. The need for experimental data

In order to make real progress on questions of cloud radiation and its relationship to the drop distribution, measurements of three types are essential:

the complete (r = 1 to 3000 μm) drop spectrum;
the spectral albedo;
the spectral transmissivity.

All three types of measurements must be made simultaneously. This is admittedly a difficult proposition. Even with the advent of Knollenberg probes that potentially give the complete drop distribution, almost no such distributions have been published. Most field programs still measure only broadband flux instead of spectral intensity, and often don't even do a very accurate job of that. But unless we start the long process of making more sophisticated measurements, we shall remain constrained to comparing one theory with another, with no idea which (if any) is correct.

REFERENCES

Deirmendjian, D., 1969: *Electromagnetic Scattering on Spherical Polydispersions.* American-Elsevier, 290 pp.

Houze, R., P. Hobbs, P. Herzegh and D. Parsons, 1979: Size distributions of precipitation particles in frontal clouds. *J. Atmos. Sci.*, **36**, 156–162.

Nussenzweig, H., and W. Wiscombe, 1980: Efficiency factors in Mie scattering. *Phys. Rev. Lett.*, **45**, 1490–1494.

Wiscombe, W., R. Welch and W. Hall, 1984: The effects of very large drops on cloud absorption. Part I: parcel models. *J. Atmos. Sci.*, **41**, 1337–1355.